

AD A 042183

HIRIS EXPERIMENT-CHATANIKA RADAR RESULTS

Technical Report 9

DNA 4229T

12

Stanford Research Institute
333 Ravenswood Avenue
Menlo Park, California 94025

January 1977

Topical Report for Period January 1976—December 1976

CONTRACT No. DNA 001-77-C-0042

APPROVED FOR PUBLIC RELEASE;
DISTRIBUTION UNLIMITED.

THIS WORK SPONSORED BY THE DEFENSE NUCLEAR AGENCY
UNDER RDT&E RMSS CODE B322076462 I25AAXHX63132 H2590D.

JUL
FILE

AD NU.
DDC FILE COPY

Prepared for
Director
DEFENSE NUCLEAR AGENCY
Washington, D. C. 20305

11

Destroy this report when it is no longer
needed. Do not return to sender.



UNCLASSIFIED

SECURITY CLASSIFICATION OF THIS PAGE (When Data Entered)

19 REPORT DOCUMENTATION PAGE		READ INSTRUCTIONS BEFORE COMPLETING FORM
1. REPORT NUMBER DNA 4229T	2. GOVT ACCESSION NO.	3. RECIPIENT'S CATALOG NUMBER
4. TITLE (and Subtitle) HIRIS EXPERIMENT—CHATANIKA RADAR RESULTS, Technical Report 9		5. TYPE OF REPORT & PERIOD COVERED Topical Report, Interim Period Jan 76—Dec 76
7. AUTHOR(s) Theodore M. Watt		6. PERFORMING ORG. REPORT NUMBER SRI Project 5915
		8. CONTRACT OR GRANT NUMBER(s) DNA 001-77-C-0042 new
9. PERFORMING ORGANIZATION NAME AND ADDRESS Stanford Research Institute 333 Ravenswood Avenue Menlo Park, California 94025		10. PROGRAM ELEMENT, PROJECT, TASK AREA & WORK UNIT NUMBERS NWET Subtask I25AAXHX631-32
11. CONTROLLING OFFICE NAME AND ADDRESS Director Defense Nuclear Agency Washington, D.C. 20305		12. REPORT DATE Jan 1977
14. MONITORING AGENCY NAME & ADDRESS (if different from Controlling Office)		13. NUMBER OF PAGES 38
15. SECURITY CLASS (of this report) UNCLASSIFIED		15a. DECLASSIFICATION/DOWNGRADING SCHEDULE
16. DISTRIBUTION STATEMENT (of this Report) Approved for public release; distribution unlimited.		
17. DISTRIBUTION STATEMENT (of the abstract entered in Block 20, if different from Report)		
18. SUPPLEMENTARY NOTES This work sponsored by the Defense Nuclear Agency under RDT&E RMSS Code B322076462 I25AAXHX63132 H2590D.		
19. KEY WORDS (Continue on reverse side if necessary and identify by block number) Incoherent-Scatter Radar Ionospheric Current Density Auroral Ionosphere Height-Integrated Conductivities Electron Density Joule Heating Ion Velocity Particle Energy Deposition Ionospheric Electric Fields E-Region Neutral Winds		
20. ABSTRACT (Continue on reverse side if necessary and identify by block number) Results of the Chatanika DNA 617 Radar support of the HIRIS rocket experiment are presented, along with magnetometer, riometer, and all-sky camera data to give a more complete picture of ionospheric processes. The HIRIS experiment took place on 1 April 1976, beginning at 0805:20 UT. The purpose of the experiment was to measure IR emissions in an aurorally disturbed ionosphere. The Chatanika radar was operated in support of the rocket experiment from 0626 UT to 0821 UT. Radar data acquired during the HIRIS experiment are presented →		

DD FORM 1473

EDITION OF 1 NOV 68 IS OBSOLETE

UNCLASSIFIED

SECURITY CLASSIFICATION OF THIS PAGE (When Data Entered)

332 500

UNCLASSIFIED

SECURITY CLASSIFICATION OF THIS PAGE(When Data Entered)

20. ABSTRACT (Continued)

in this report. In general, the following results were obtained:

- Background electron densities in the vicinity of the rocket trajectory ranged between 3×10^3 and $3 \times 10^5 \text{ cm}^{-3}$. During the background measurement period (<0745 UT) the peak of the auroral-E layer appeared to be above the trajectory apogee with electron densities at all altitudes fluctuating with time. Horizontal gradients in density were observed from about 0700 to 0730 UT and seemed consistent with a density enhancement moving geomagnetically west. During the elevation-scan measurements just prior to launch the peak of the ionization layer varied from 100 to 120 km and ionization density continued to fluctuate with time.
- Vector quantities measured during the prelaunch background period were indicative of the active conditions present during the experiment. Conductivities, current densities, neutral winds and electric fields all tended to be unipolar during the measurement period, but exhibited large peaks centered at about 0640 and 0730 UT.
- Electron densities along the rocket trajectory, as measured by the radar, were typically $\leq 2 \times 10^5/\text{cm}^3$.
- Energy spectra of precipitating electrons during the rocket flight had characteristic energies of 1.5 to 3 keV and total energy fluxes of 6 to 10 ergs/cm²/s.

UNCLASSIFIED

SECURITY CLASSIFICATION OF THIS PAGE(When Data Entered)

PREFACE

The author wishes to express his appreciation to John D. Kelly, who operated the Chatanika Radar during the HIRIS experiment and to Mary A. McCready and Barbara J. Phillips who reduced the on-line data.

Thanks also go to Drs. M. Baron, R. Vondrak, and P. Perreault, and Mr. J. Spencer for many helpful suggestions in preparing this report.

Data used in connection with this report were obtained from the Geophysical Institute at Fairbanks, Alaska, from WDC-A for Solar Terrestrial Physics (Geomagnetism), Boulder, Colorado, and from Space Data Corporation, Phoenix, Arizona.

ACCESSION for	
NTIS	Write Section
DDC	Diff Section
UNANNOUNCED	<input checked="" type="checkbox"/>
JUSTIFICATION	<input type="checkbox"/>
BY	
DISTRIBUTION/AVAILABILITY CODES	
Dist.	AVAIL. and/or SPECIAL
<input checked="" type="checkbox"/>	<input type="checkbox"/>

CONTENTS

PREFACE	1
I INTRODUCTION	5
II BACKGROUND MEASUREMENTS.	7
A. Geomagnetic Conditions.	7
B. Auroral Conditions.	7
C. Absorption.	7
D. Electron Density.	10
1. Three-Position Measurements.	10
2. Elevation-Scan Measurements.	13
E. Height-Integrated Conductivities.	14
F. Electric Field.	16
G. Neutral Wind.	17
H. Height-Integrated Current Density	18
I. Energy Deposition	19
III CORRELATED MEASUREMENTS.	21
A. General	21
B. Separation Between Rocket and Radar Beam.	21
C. Electron Density.	22
D. Energy Spectra of Precipitating Electrons	24
E. Volume Energy Deposition	26
IV SUMMARY AND CONCLUSIONS.	29
REFERENCES	31

ILLUSTRATIONS

1	H-Component Magnetograms on 1 April 1976 from Two Stations Distributed in Latitude but in the Same Local Time Sector as the Rocket Trajectory	8
2	All-Sky Photographs for the Period 0720 UT through 0820 UT, 1 April 1976.	9
3	College Riometer Records for 30 March and 1 April 1976	10
4	Background Contours of Electron Density for the HIRIS Experiment on 1 April 1976	11
5	Electron Density versus Time at Radar Antenna Azimuth Angles of 30°, 90°, and 330°, and at Altitudes of 120 km (a) and 110 km (b), Illustrating the Presence of Horizontal Gradients.	12
6	Meridian-Plane Map of Electron Density Contours Based on Radar Observations from 0801:37 to 0803:52 UT, 1 April 1976	14
7	Meridian-Plane Map of Electron Density Contours and Rocket-Induced Echoes Based on Radar Observations from 0803:52 to 0806:07 UT, 1 April 1976.	15
8	Height-Integrated Conductivities for the HIRIS Experiment on 1 April 1976	16
9	Electric Field for the HIRIS Experiment on 1 April 1976	17
10	Height-Averaged E-Region Neutral Wind for the HIRIS Experiment on 1 April 1976	18
11	Height-Integrated Current Density for the HIRIS Experiment on 1 April 1976	19
12	Joule Heating and Energetic Particle Contributions to Total Energy Deposition for the HIRIS Experiment on 1 April 1976.	20
13	Illustration of Horizontal Separation Between the Radar Beam and the Rocket for the HIRIS Experiment on 1 April 1976.	22
14	Electron Density as Functions of Time and Altitude During the HIRIS Flight, Along with Both Real and Apparent Trajectories of the Rocket.	23
15	Energy Spectra of Auroral Electrons and Associated Electron-Density Profiles for the Periods 0801:37 to 0801:52 UT and 0804:53 to 0804:59 UT, 1 April 1976	25

16	Volume Energy Deposition Rate in the Vicinity of the HIRIS Trajectory for the Period 0801:37 to 0803:47 UT, 1 April 1976	27
17	Volume Energy Deposition Rate in the Vicinity of the HIRIS Trajectory for the Period 0803:52 to 0806:06 UT, 1 April 1976	28

I INTRODUCTION

The DNA-AFGL HIRIS (High Resolution Interferometer Spectrometer) was successfully launched from Poker Flat, Alaska at 0805:20 UT, 1 April 1976.^{1*} A Sergeant rocket carried the payload to an apogee of 125.6 km at 175 s after launch. The payload was above 70 km altitude during the interval 72 s to 288 s after launch. The purpose of the HIRIS experiment was to obtain high-resolution data on the infrared emissions of an aurorally disturbed ionosphere in the 4-to-16- μ m wavelength range. The primary instrument in the payload was a cryogenically cooled Michelson interferometer.

The Chatanika radar was operated in support of the rocket experiment from 0626 UT to 0821 UT. From 0626 UT to 0745 UT, the radar antenna was operated successively at three positions using azimuth/elevation angles of $330^{\circ}/80^{\circ}$, $30^{\circ}/60^{\circ}$, and $90^{\circ}/80^{\circ}$. Each position was maintained for two minutes, and a sequence of three positions was accomplished in six minutes. The three-position mode of operation permitted measurement of transport quantities (electric field, current density, and neutral wind), and the particular arrangement of antenna positions caused the region interrogated by the radar to be near the ionospheric part of the rocket trajectory.

From 0801:37 UT to 0806:07 UT, the radar was operated in an elevation scan mode, at an azimuth angle of 44° , in order to provide more precise information on electron densities near the expected rocket trajectory just prior to launch. The first scan started at 0801:37 UT, 35° elevation angle. The second scan started at 0803:52 UT, 90° elevation angle, and ended at 0806:07 UT, 36° elevation angle.

*References are listed at the end of the report.

At 0806:07 UT, before the rocket reached the ionospheric part of its path, the radar antenna was placed at 44° azimuth, 63° elevation. This position placed the antenna beam nearly tangent to a section of the upleg trajectory, yielding nearly collocated radar and rocket measurements during this portion of the flight. At 0808:51 UT, the radar antenna was repositioned to 44° azimuth, 43° elevation, thus providing near intersection with a point on the downleg trajectory. Details of the geometry are discussed more fully in Section III.

At the time of the HIRIS experiment, a well-developed ionospheric storm was in progress. Initial disturbances on 1 April were observed on College magnetograms about 0200 UT, and by the time of the rocket launch, geomagnetic, auroral, absorption, and electron density observations all indicated very active conditions. These conditions satisfied the requirements of the HIRIS experiment, which was to study IR emissions from bright aurora.

II BACKGROUND MEASUREMENTS

A. Geomagnetic Conditions

Geomagnetic conditions were disturbed both before and during the experiment. Figure 1 illustrates H-component magnetograms for the period 0600 to 1000 UT on 1 April 1976 from Honolulu and College. These stations are at different latitudes but are in the same local time sector. The baseline curve for each magnetogram was taken from pre-storm measurements for the period 1900 to 2300 UT, 31 March 1976.

Both magnetograms illustrate the effects of the storm. The Honolulu magnetogram exhibits substorm-related fluctuations of ~ 5 γ , and the College magnetogram, reflecting conditions directly beneath active aurora, exhibits substorm-related fluctuations >100 γ , during the period of interest. The magnetogram from Sitka, also in the same local time sector, also indicated large fluctuations, but is not illustrated here because the readings were mostly off-scale.

B. Auroral Conditions

Brilliant and dynamic auroral displays characterized the night of 1 April 1976. Figure 2 illustrates all-sky photographs taken at Chatanika from 0720 UT to 0820 UT. The photographs display conditions at one-minute intervals during the HIRIS flight (0805 to 0811 UT) and at five-minute intervals before and after the flight.

C. Absorption

Figure 3 illustrates absorption measured by the College riometer for the period 0700 to 0900 UT on 1 April 1976. The same time period for 30 March 1976 is also presented as a quiet-day reference. By comparing the records for the two days it can be seen that absorption on 1 April was enhanced well before the HIRIS flight occurred. At about 0757 UT,

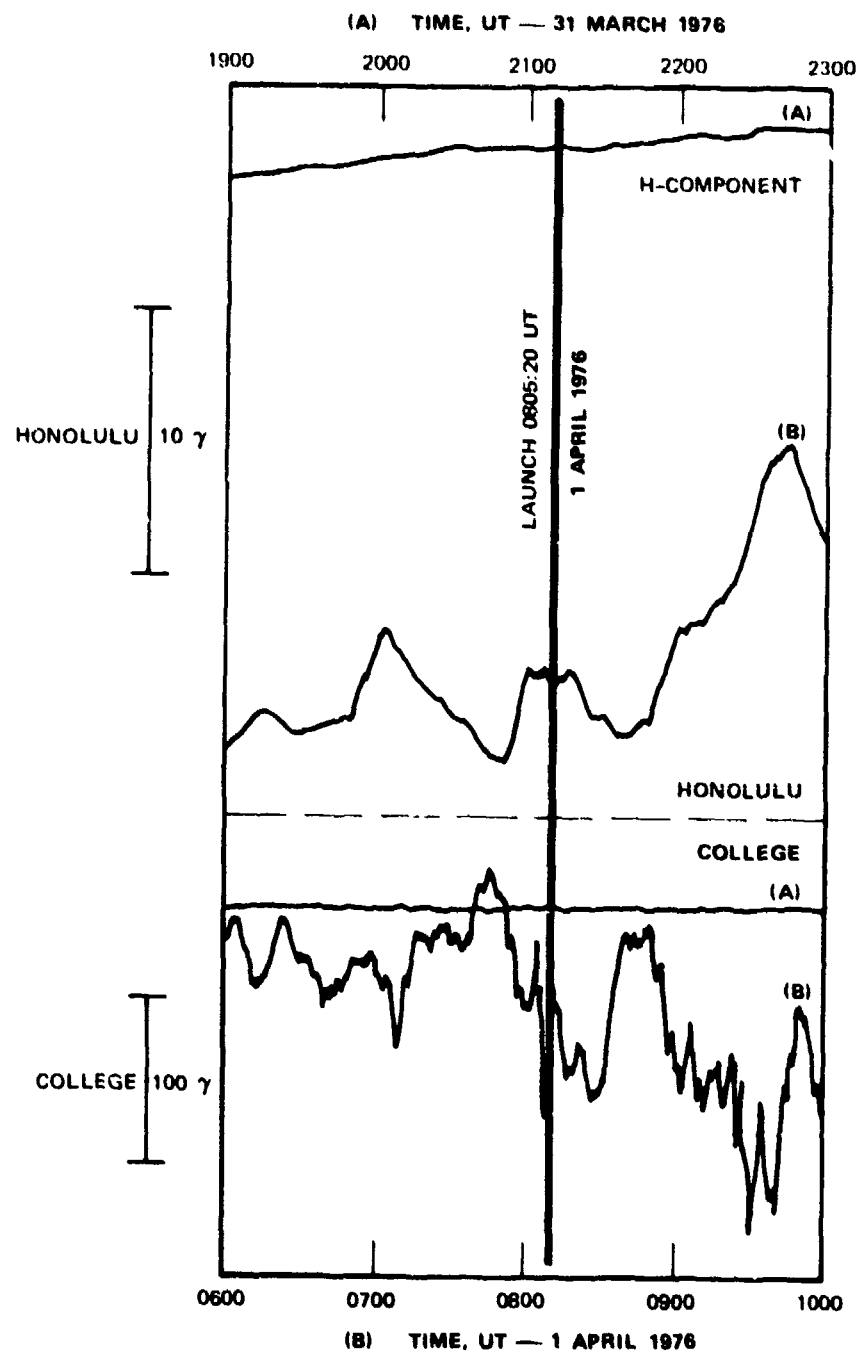
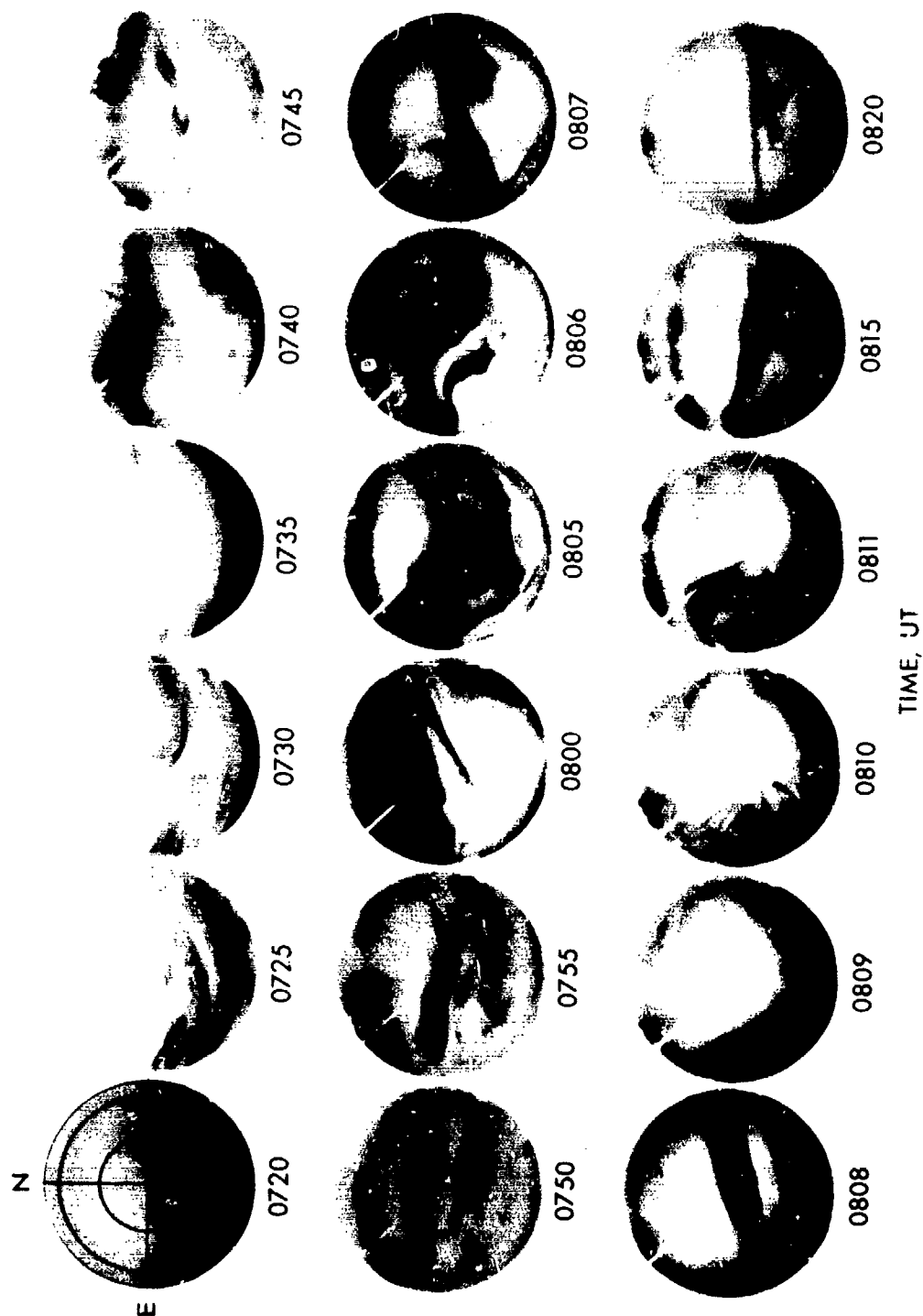


FIGURE 1 H-COMPONENT MAGNETOGRAMS ON 1 APRIL 1976 FROM TWO STATIONS DISTRIBUTED IN LATITUDE BUT IN THE SAME LOCAL TIME SECTOR AS THE ROCKET TRAJECTORY



LA-5915-2

FIGURE 2 ALL-SKY PHOTOGRAPHS FOR THE PERIOD 0720 UT THROUGH 0820 UT, 1 APRIL 1976

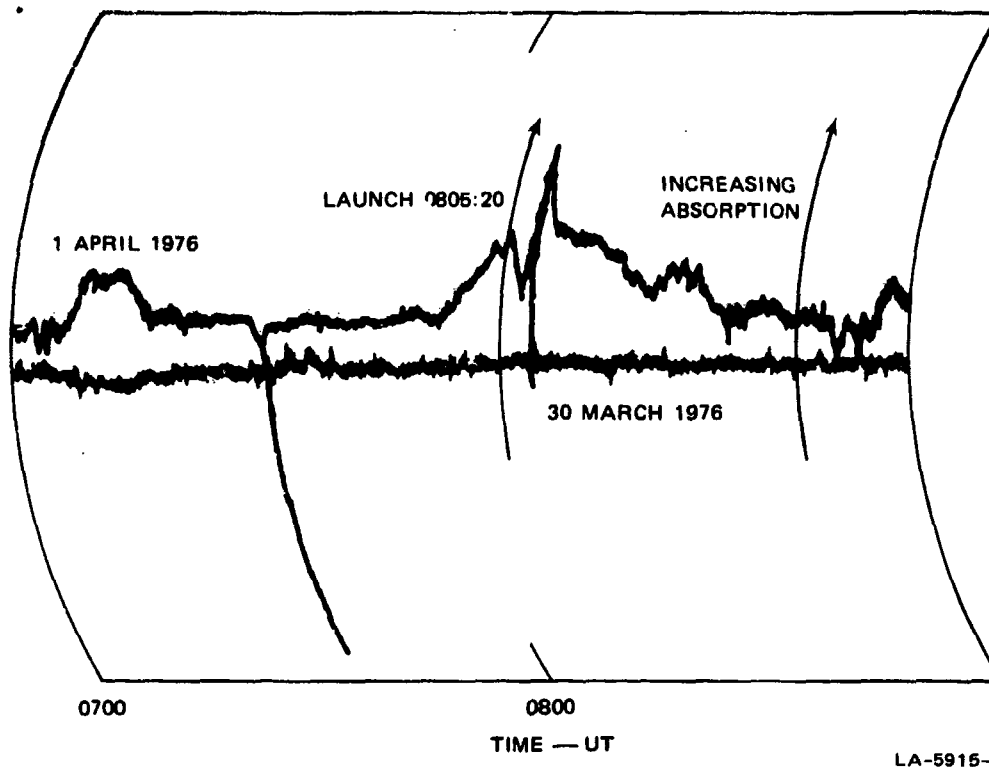


FIGURE 3 COLLEGE RIOMETER RECORDS FOR 30 MARCH AND 1 APRIL 1976

absorption began to increase further. Thereafter, absorption was high and irregular throughout the rocket flight.

D. Electron Density

1. Three-Position Measurements

It was stated earlier that, prior to the HIRIS flight, the Chatanika radar was operated in two antenna modes--a three-position mode requiring about six minutes for a complete sequence, and an elevation-scan mode requiring slightly over two minutes for each scan. The two modes provided separate and complimentary forms of background electron density for the HIRIS experiment.

Figure 4 presents the temporal behavior of spatially averaged electron densities observed by the radar from 0626 UT to 0745 UT, while the radar was operating in the three-position mode. Each data point represented an average of a measurement at each of the three antenna

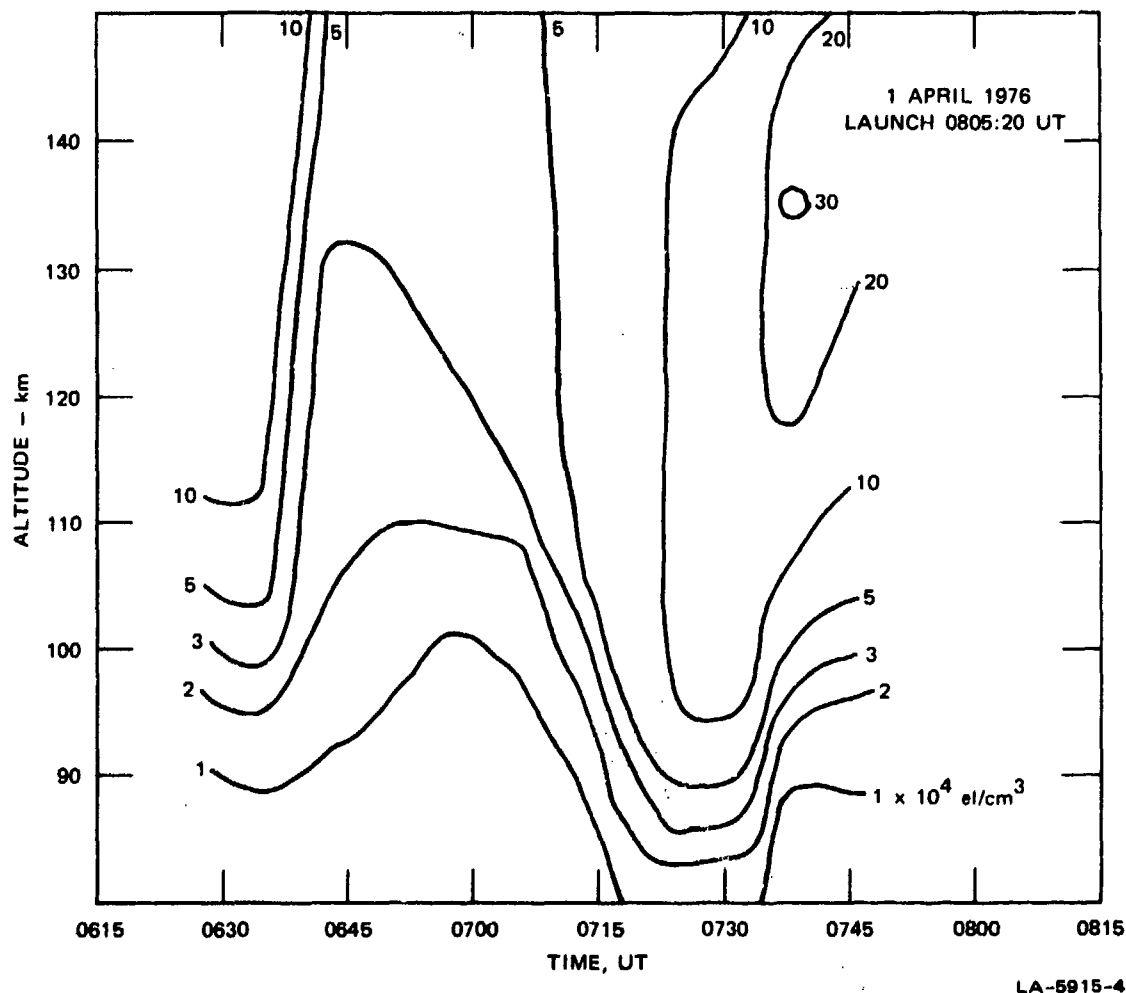
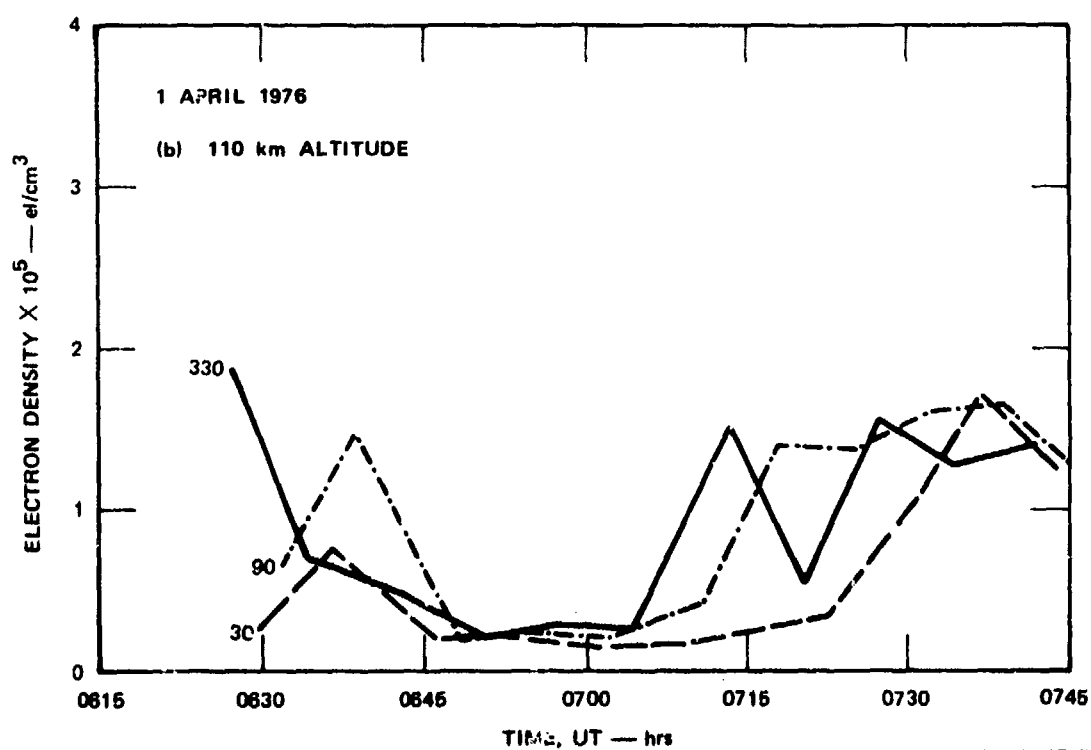
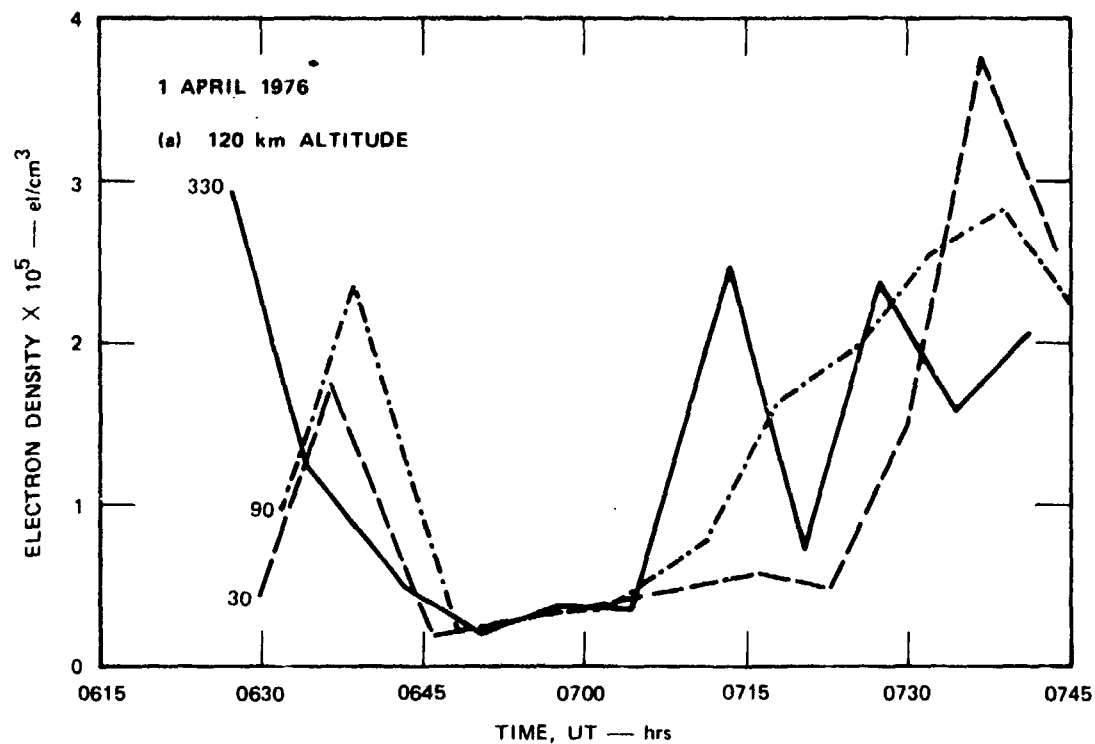


FIGURE 4 BACKGROUND CONTOURS OF ELECTRON DENSITY FOR THE HIRIS EXPERIMENT ON 1 APRIL 1976

positions, and smooth contours were then drawn through the data. The figure shows density enhancement occurring from 0715 UT to 0735 UT below 100 km altitude and another enhancement beginning at about 0735 UT above about 120 km altitude. Because Figure 4 presents spatially averaged data, it provides us no information on horizontal gradients in electron density that may have existed.

The importance of horizontal gradients in electron density may be assessed by considering the time histories of electron density observations made at each of the three antenna positions separately. Figure 5 presents examples of such time histories at 120 km and 110 km altitude.



LA-5915-5

FIGURE 5 ELECTRON DENSITY vs TIME AT RADAR ANTENNA AZIMUTH ANGLES OF 30°, 90°, AND 330°, AND AT ALTITUDES OF 120 km (a) AND 110 km (b), ILLUSTRATING THE PRESENCE OF HORIZONTAL GRADIENTS

The three antenna positions are indicated by their azimuth angles of 30° , 90° , and 330° .

Figure 5 indicates that from 0648 UT to 0704 UT there was little or no horizontal gradient in electron density present within the area circumscribed by the antenna positions. At 0704 UT a large, horizontal gradient began to form. Except for the large density observed at 0714 UT on 330° azimuth, the general trend from 0704 UT to 0730 UT seems to be associated with a density enhancement moving in a generally westerly direction. In particular, the observed behavior from 0704 UT to 0739 UT is consistent with an enhancement moving at about 190 m/s in a direction of about 76° east of north. This estimate is quite approximate because of the small quantity of data available, but it demonstrates a capability of the radar that could be used in future experiments.

2. Elevation-Scan Measurements

Background electron densities for the HIRIS experiment were also obtained in the form of elevation-scan measurements. These measurements provided altitude-versus-ground-range contours of electron density in a vertical plane passing through the radar. For the HIRIS experiment, the elevation scans were performed at an azimuth bearing of 44° so that the plane of the antenna scans would lie close to the expected trajectory of the rocket.

Figures 6 and 7 illustrate contours of electron density obtained from elevation scans occurring just before the rocket flight. Also plotted on each figure is the projection of the expected trajectory of the rocket onto the plane of the antenna scan. It will be shown in Section III that the plane of the HIRIS rocket trajectory and the plane of the antenna scan were nearly parallel and separated by less than 10 km during most of the rocket flight (see Section III-E, Figure 13). Figures 6 and 7 thus provide a description of ionospheric electron densities that existed near the expected path of the rocket just prior to the rocket flight.

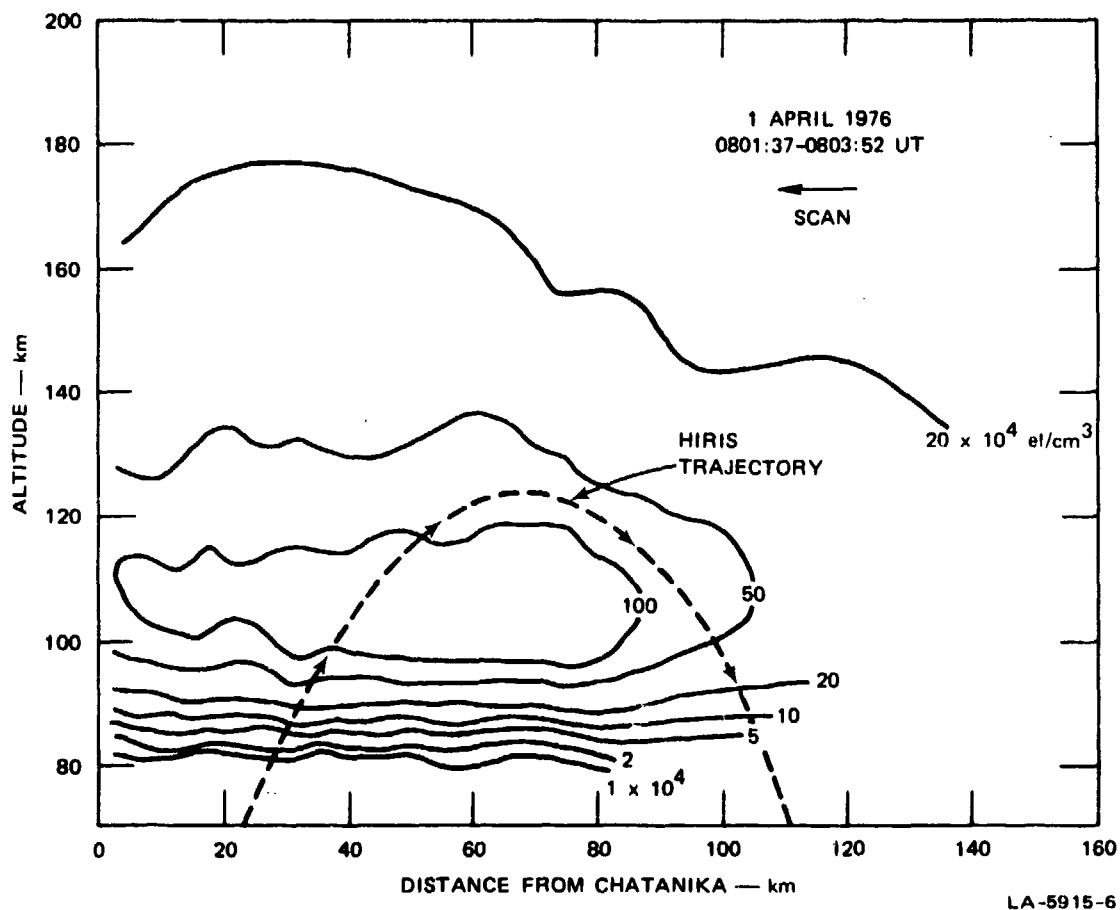


FIGURE 6 MERIDIAN-PLANE MAP OF ELECTRON DENSITY CONTOURS BASED ON RADAR OBSERVATIONS FROM 0801:37 TO 0803:52 UT, 1 APRIL 1976

Figure 6 indicates electron densities $>10^6/\text{cm}^3$ between 100 and 120 km altitude along the upleg portion of the trajectory about two minutes before launch. Figure 7 indicates electron densities $>10^6/\text{cm}^3$ between 100 and 110 km altitude along the downleg portion of the trajectory occurring about launch time. The differences between Figures 6 and 7 are indicative of the dynamic conditions present during the HIRIS experiment.

E. Height-Integrated Conductivities

Figure 8 illustrates the Hall and Pedersen conductivities measured during the three-position mode of the radar (0626 UT to 0745 UT). Hall conductivity is shown by the dashed line and Pedersen conductivity by the solid line. Conductivities were not calculated while the antenna was

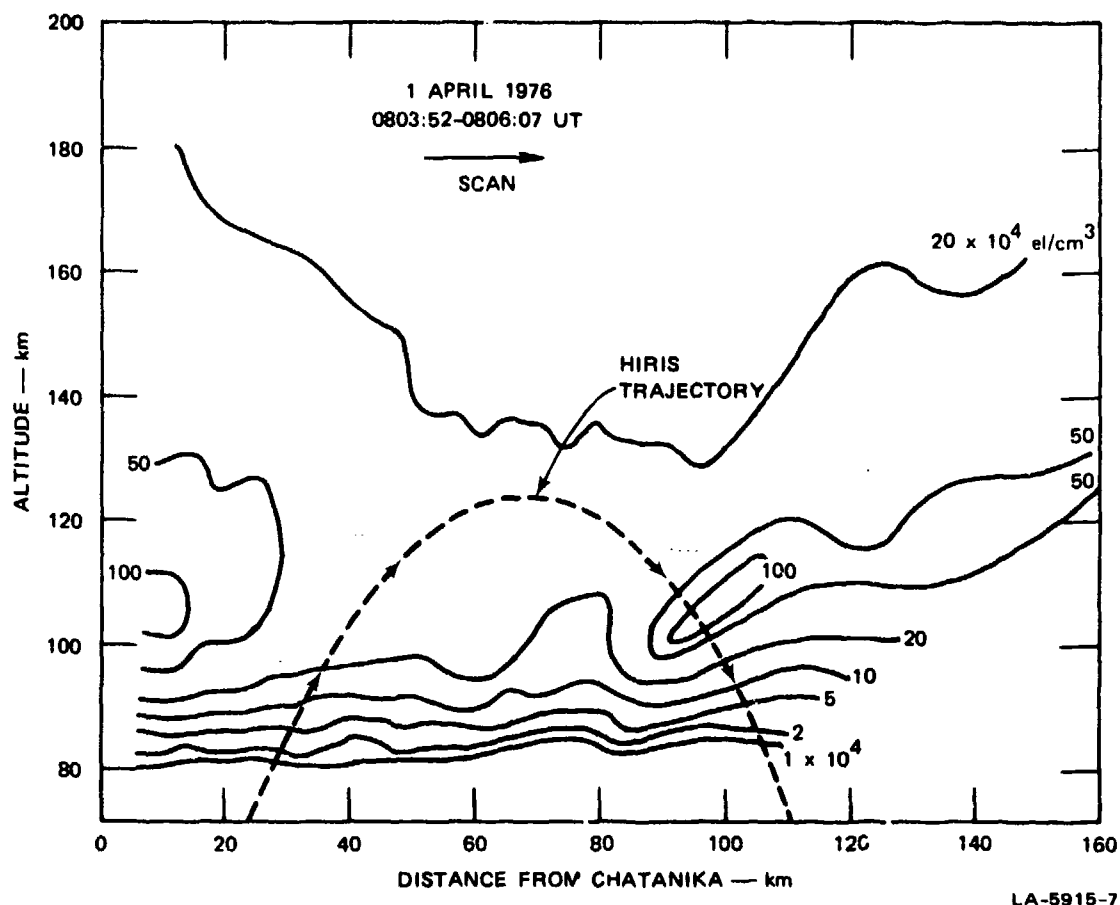


FIGURE 7 MERIDIAN-PLANE MAP OF ELECTRON DENSITY CONTOURS AND ROCKET-INDUCED ECHOES BASED ON RADAR OBSERVATIONS FROM 0803:52 TO 0806:07 UT, 1 APRIL 1976

operating in an elevation-scan mode. As expected, both conductivities, which are proportional to electron density, exhibited a temporal behavior similar to that of electron density during the same time period. By comparing Figures 4 and 8 it can be seen that the general behavior of both conductivities agrees with the behavior of the spatially averaged densities observed by the radar.

The detailed behavior of the curves in Figure 8 illustrates the inhomogeneous nature of the conductivities in the presence of horizontal density gradients. Each data point calculated for Figure 8 corresponds to a single antenna position, and it can be seen that conductivities vary from position to position, consistent with the density variations illustrated in Figure 5.

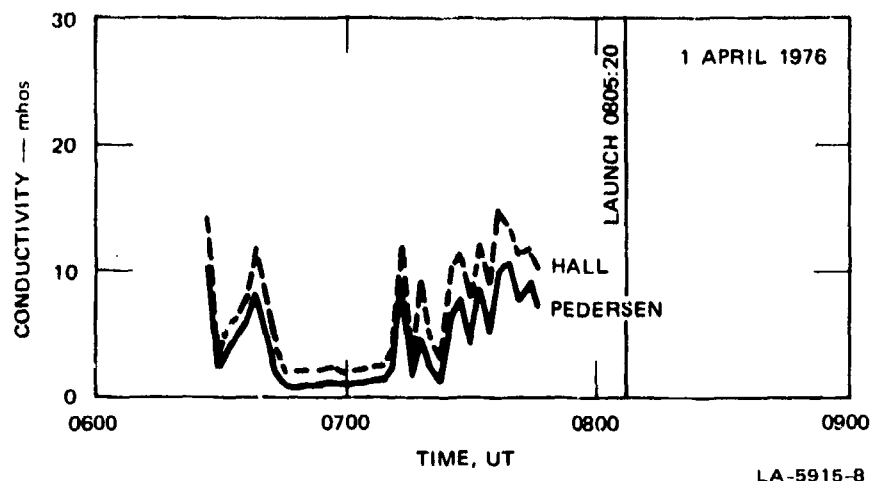


FIGURE 8 HEIGHT-INTEGRATED CONDUCTIVITIES FOR THE HIRIS EXPERIMENT ON 1 APRIL 1976

During the period 0626 UT to 0745 UT, Figure 8 shows that Hall conductivity varied between 2 and 15 mhos, and Pedersen conductivity varied between 1 and 10 mhos.

F. Electric Field

The ionospheric electric field, as determined from data taken in the 225-km-altitude range gate, is presented in Figure 9 for the period 0626 UT to 0745 UT. The geomagnetic north-south component is shown by the dashed line, and the east-west component is shown by the solid line. The data shown were acquired while the radar was operating in a three-position mode. No electric field measurements were obtained while the radar was operating in an elevation-scan mode.

During the period shown, a consistent westward component of electric field was present, varying from 1 to 76 mV/m, and with an average value of about 30 mV/m. The north-south component was directed mostly toward the south but exhibited three short fluctuations toward the north during the time period examined. The maximum amplitude of the north-south component was 82 mV/m southward and the average amplitude was about 40 mV/m southward.

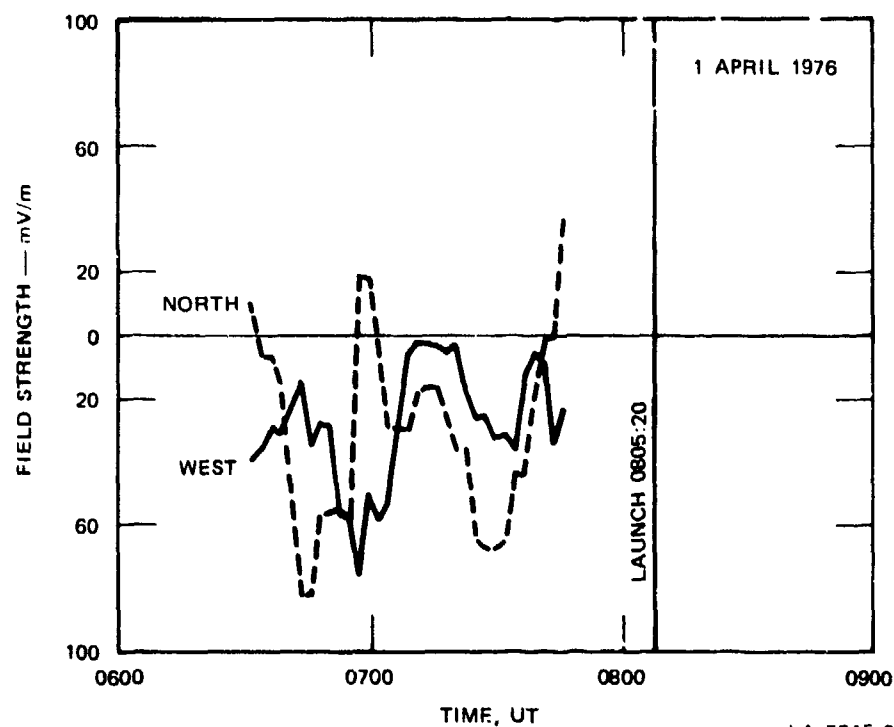
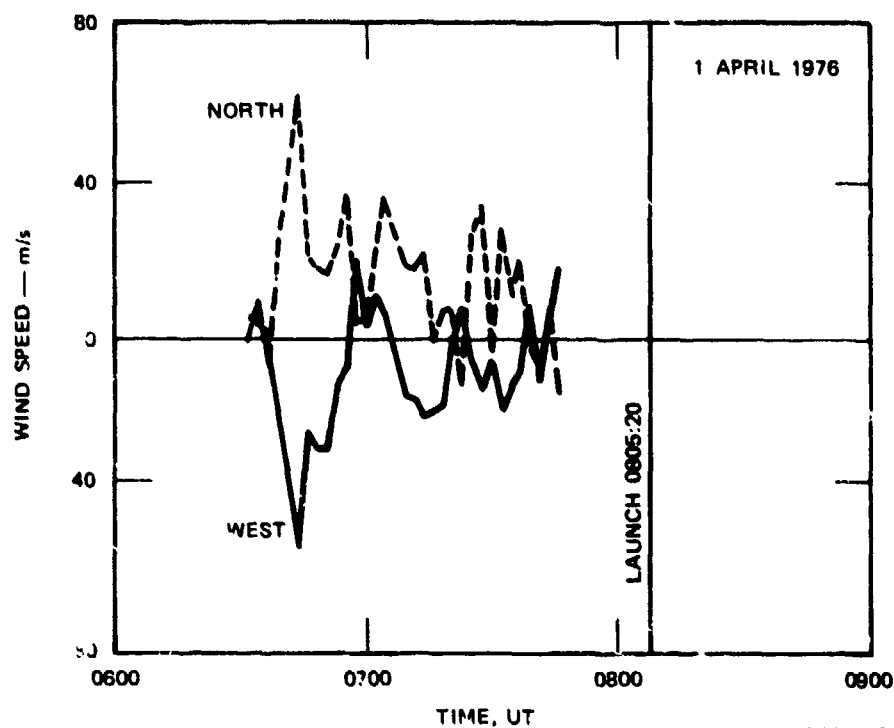


FIGURE 9 ELECTRIC FIELD FOR THE HIRIS EXPERIMENT ON 1 APRIL 1976

G. Neutral Wind

The E-region horizontal neutral wind was computed using the method described by Baron and Chang.^{2,3} The neutral wind computed by this method represents a weighted average over 40 to 50 km of altitude, but the radar measurements are heavily weighted toward the altitude of peak electron density. As the altitude of the peak density changes, apparent temporal changes in neutral wind may simply represent changes in the altitude at which the neutral wind is being sampled. In addition, the accuracy becomes poor at low SNR.

Figure 10 shows the E-region neutral-wind estimates as a function of time. The measurements of neutral wind were made from 0626 to 0745 UT, while the antenna was operating in a three-position mode. The neutral-wind estimates between 0626 and 0700 UT are probably the least releable because the electron density and SNR were lowest during this period (see Figure 4). During this time period there was a northward component of



LA-5915-10

FIGURE 10 HEIGHT-AVERAGED E-REGION NEUTRAL WIND FOR THE HIRIS EXPERIMENT ON 1 APRIL 1976

about 40 ± 20 m/s and a westward component varying from 0 to 60 m/s. The magnitudes of both components tended to decrease after about 0700 UT.

H. Height-Integrated Current Density

Figure 11 illustrated height-integrated current density components for the period of three-position radar operations.^{4,5} No measurements of current density were made while the radar antenna was operating in an elevation-scan mode.

Peaks of westward current density of about 1 A/m occurred near 0650 and 0735 UT. Except for these peaks, both components of current density were small--less than ± 0.4 A/m during the measurement period.

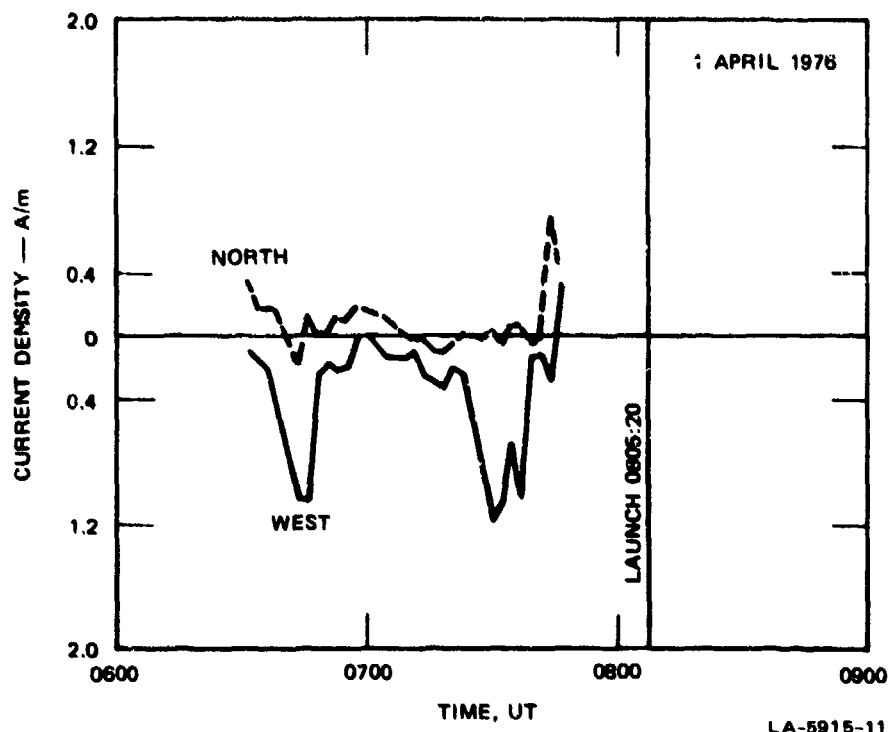


FIGURE 11 HEIGHT-INTEGRATED CURRENT DENSITY FOR THE HIRIS EXPERIMENT ON 1 APRIL 1976

1. Energy Deposition

The calculated energy deposited from joule heating is shown in Figure 12.² Calculations of joule heating were made only from 0626 to 0745 UT while the antenna was operating in a three-position mode.

Peaks of joule heating of 30 to 35 $\text{ergs/cm}^2/\text{s}$ occurred near 0650 and 0735 UT, consistent with peaks of current shown in Figure 11. Except for these peaks, joule heating during the observation period was less than 10 $\text{ergs/cm}^2/\text{s}$.

Figure 12 also shows the rate of energy deposition by the precipitating electrons as a function of time.^{5,6} Throughout the measurement period, energy deposition by precipitating electrons was less than 7 $\text{ergs/cm}^2/\text{s}$, with an average value of perhaps 2 to 3 $\text{ergs/cm}^2/\text{s}$.

Total average energy deposition due to both sources was about 10 to 15 $\text{ergs/cm}^2/\text{s}$ during the period of the rocket experiment.

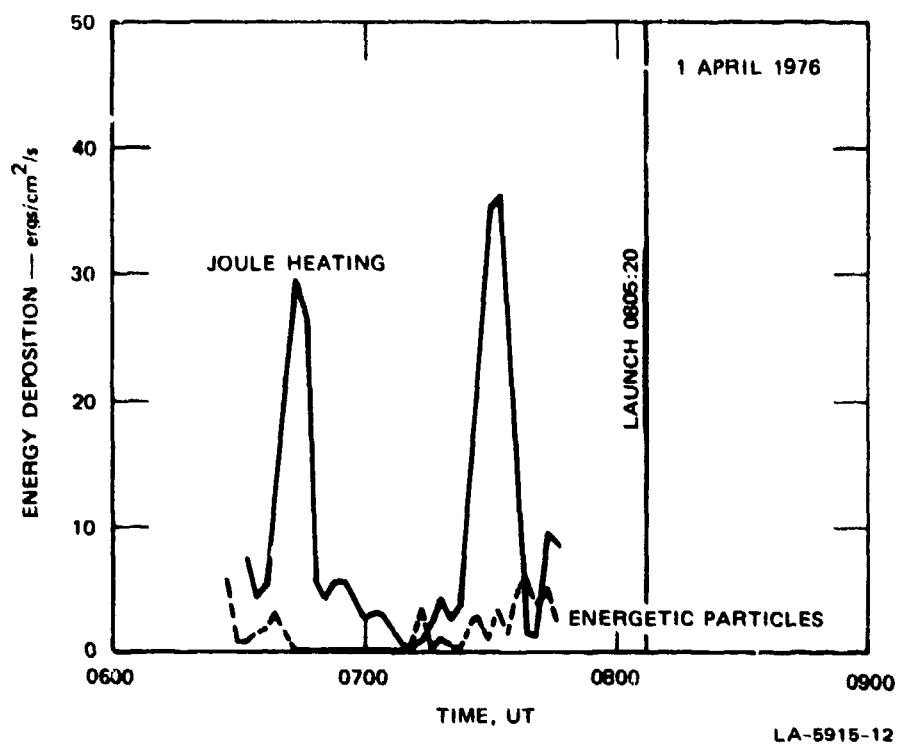


FIGURE 12 JOULE HEATING AND ENERGETIC PARTICLE CONTRIBUTIONS TO TOTAL ENERGY DEPOSITION FOR THE HIRIS EXPERIMENT ON 1 APRIL 1976

III CORRELATED MEASUREMENTS

A. General

The HIRIS rocket was launched at 0805:20 UT. At this time the Chatanika radar was operating in an elevation-scan mode, as described in Section II-D-2, and providing background density information in the vicinity of the expected trajectory of the rocket. At 0806:07 UT, the radar antenna was moved to a fixed position of 44° azimuth, 63° elevation, in order to provide correlated measurements along the upleg of the rocket flight. The rocket reached apogee at about 0808:20 UT, and at 0808:51 UT the radar antenna was repositioned to 44° azimuth, 43° elevation, in order to provide correlated measurements along the downleg of the rocket flight.

B. Separation Between Rocket and Radar Beam

Figure 13 presents a plan view of the horizontal separation between the rocket and the radar beam as the rocket traversed the ionosphere. The points along the traces marked "Radar Beam" indicate the time, in seconds, after launch of the rocket. Corresponding points are indicated along the trace marked "Rocket Trajectory," and, in addition, the numbers in parentheses indicate the instantaneous altitude, in kilometers, of the rocket at each of the times after launch. It can be seen, for example, that at 70 s after launch, the rocket was at an altitude of 68.6 km, and at this altitude the rocket was about 10 km due west of the radar beam. At 210 s after launch, the rocket was at an altitude of 120.7 km, and at this altitude, the rocket was about 50 km southwest of the radar beam. It can be seen that on the downleg of the trajectory the closest approach between the rocket and the radar beam occurred at about 260 s after launch, near 93 km altitude.

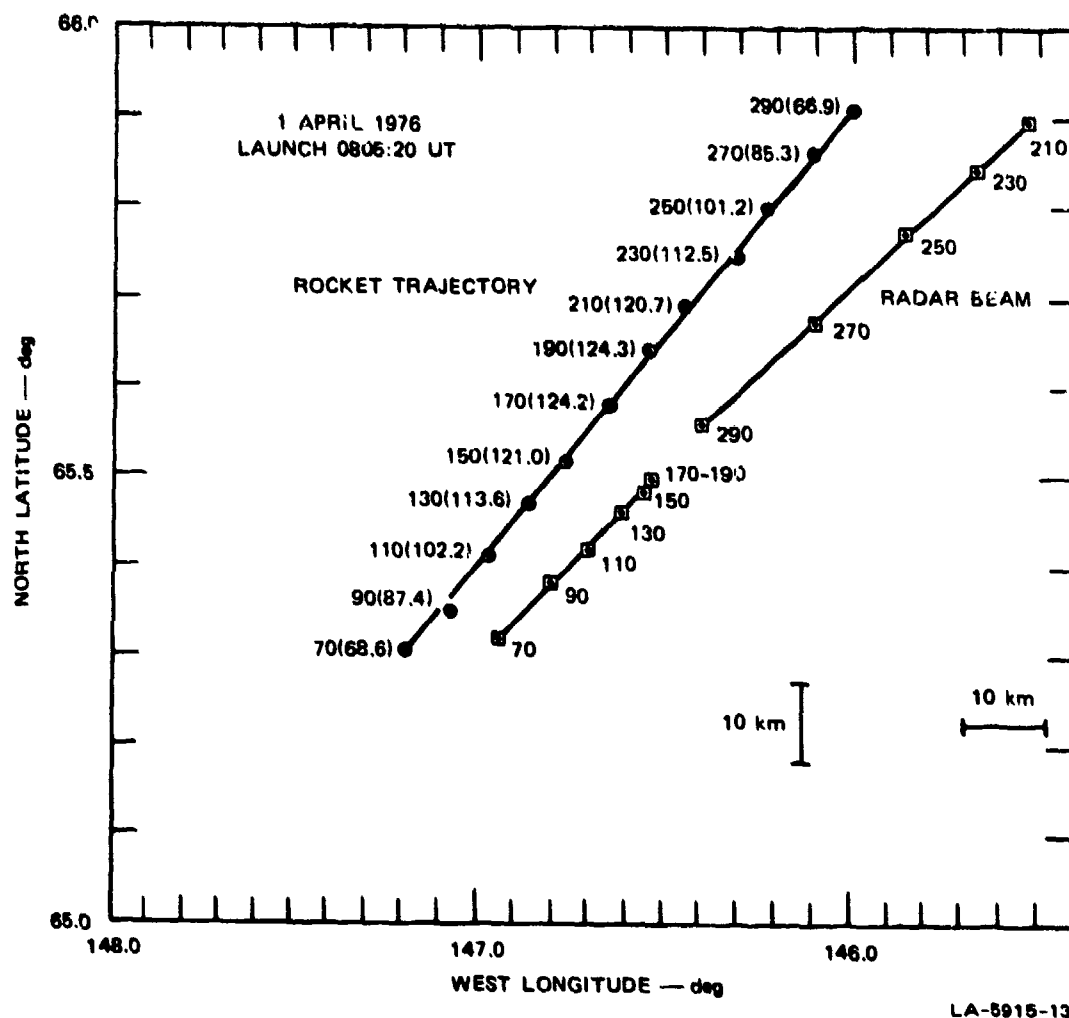


FIGURE 13 ILLUSTRATION OF HORIZONTAL SEPARATION BETWEEN THE RADAR BEAM AND THE ROCKET FOR THE HIRIS EXPERIMENT ON 1 APRIL 1976

C. Electron Density

Figure 14 illustrates contours of electron density measured during the flight of the rocket. The figure also illustrates, in altitude-time space, the actual trajectory of the rocket, and the apparent trajectory of the rocket. It has been shown in earlier reports^{7,8} that the apparent trajectory of a rocket is the locus of radar-measured rocket echoes. A rocket with an actual trajectory given by $H(t)$, where H is altitude and t is time, will give rise to an apparent trajectory of $H_a(t) = R(t) \sin \beta$, where R is the instantaneous range of the rocket from the radar, and β is the elevation angle of the radar antenna. The significance of the apparent trajectory is that it defines the possible locations of rocket-

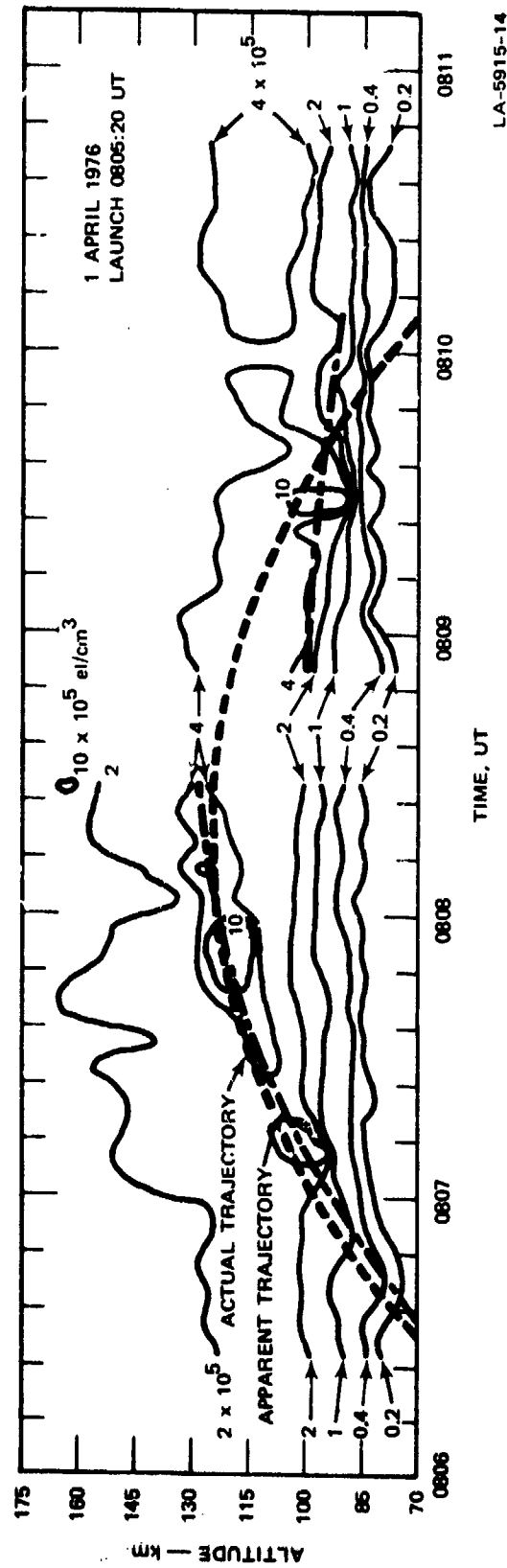


FIGURE 14 ELECTRON DENSITY AS FUNCTIONS OF TIME AND ALTITUDE DURING THE HIRIS FLIGHT, ALONG WITH BOTH REAL AND APPARENT TRAJECTORIES OF THE ROCKET

induced echoes that may appear as unwanted artifacts in a measurement of ionospheric electron density.

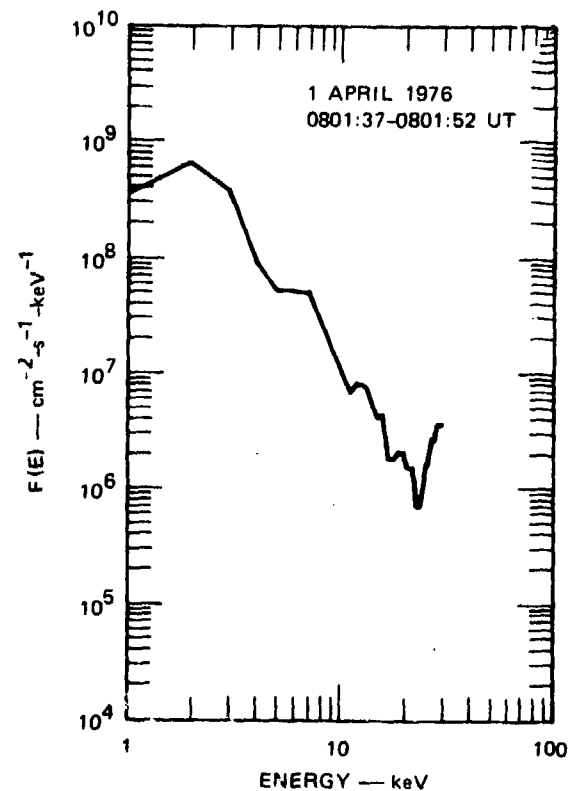
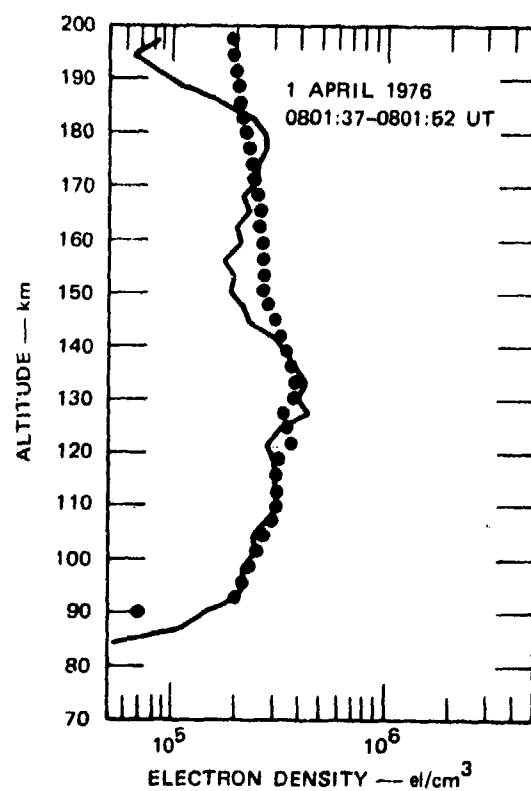
As stated earlier, the radar antenna was first pointed in one direction to provide near intersection with the rocket trajectory along the upleg portion of the flight, and was then repositioned to provide near intersection with the rocket trajectory along the downleg portion of the flight. Figure 14 illustrates that the apparent trajectory of the rocket is discontinuous, reflecting the change in antenna position during the flight.

Examination of Figure 14 reveals apparent enhancements in electron density at 0807:12, 0807:50, and 0809:30 UT, but in our judgment these are artifacts caused by rocket echoes and should be disregarded. This judgment is based in part on the fact that these apparent enhancements exist only along the apparent trajectory of the rocket in an otherwise quiet ionosphere.

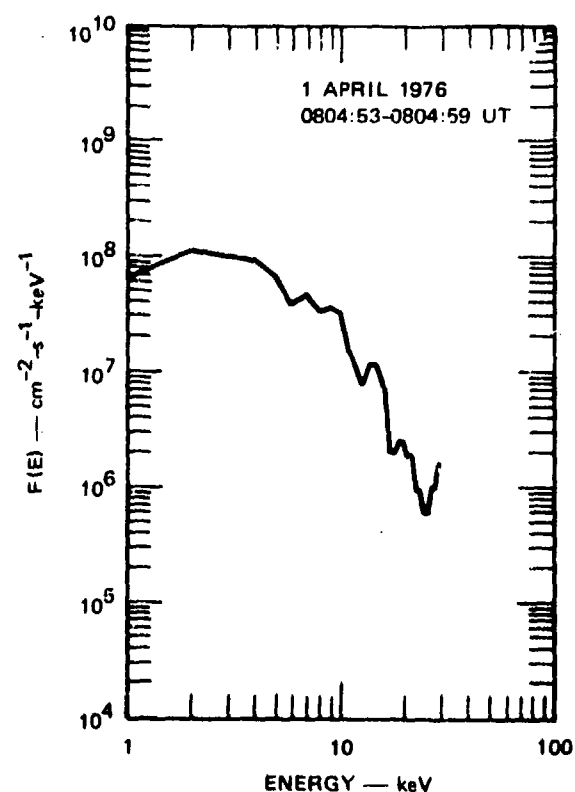
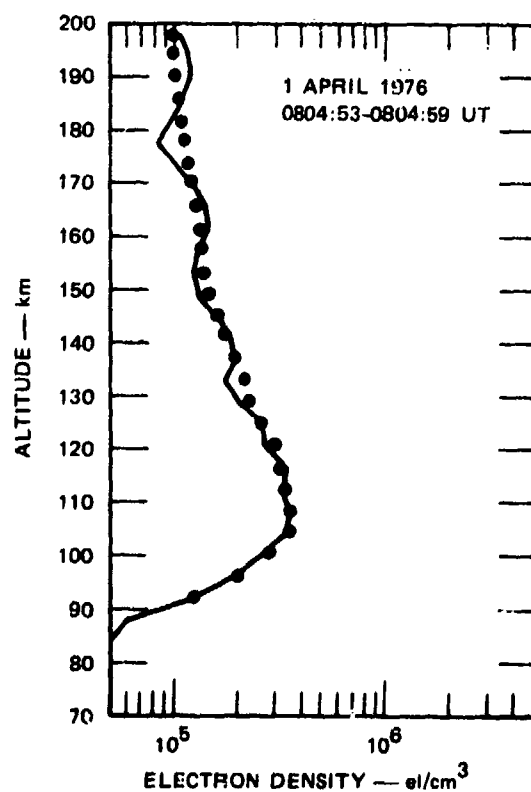
If we ignore the apparent density enhancements just discussed, then we may conclude that the rocket encountered electron densities as great as 4×10^5 el/cm³ as it traversed the E-region ionosphere.

D. Energy Spectra of Precipitating Electrons⁷

Energy spectra of precipitating electrons have been calculated for two times just prior to the HIRIS launch. Figure 15 illustrates the results of these calculations. Each calculation is presented in terms of the measured electron density profile (solid curve), and the derived electron density profile (dotted curve) that would be produced by the derived electron energy distribution. The energy spectrum in Figure 15(a) was measured slightly poleward of the HIRIS trajectory and is probably representative of the bright background aurora. The energy distribution is similar to that of a Maxwellian distribution with a characteristic energy of about 1.5 keV. The mean energy is approximately 3.2 keV and the total energy flux is $9.4 \text{ ergs/cm}^2/\text{s}$. The energy spectrum in Figure 15(a) corresponds to ionospheric conditions along the HIRIS upleg (see Figure 7). Here the incoming electron spectrum is more energetic,



(a)



(b)

LA-5915-15

FIGURE 15 ENERGY SPECTRA OF AURORAL ELECTRONS AND ASSOCIATED ELECTRON-DENSITY PROFILES FOR THE PERIODS 0801:37 TO 0801:52 UT AND 0804:53 TO 0804:59 UT, 1 APRIL 1976

although the fluxes are smaller. The distribution is similar to a Maxwellian with characteristic energy of about 3 keV. The mean energy is approximately 5.8 keV and the total energy flux is $6.5 \text{ ergs/cm}^2/\text{s}$.

E. Volume Energy Deposition

The radar-measured electron density profiles can be used to determine the spatial variation of energy input by the incoming auroral electrons. In steady-state conditions the volume energy input ϕ_E is equal to the energy required to prevent a net recombination of the ionization present and is given by the relation:

$$\phi_E = k\alpha n^2$$

where α is the effective recombination coefficient and k is 35 eV. By assuming an altitude profile of α it is possible to transform the contours of electron density in Figures 6 and 7 into contours of volume rate of energy deposition, as shown in Figures 16 and 17, respectively.

The volume energy deposition is important for computing other quantities such as optical or infrared emissions. In addition, its altitude variation can be used to obtain the energy distribution of the incoming auroral electrons.

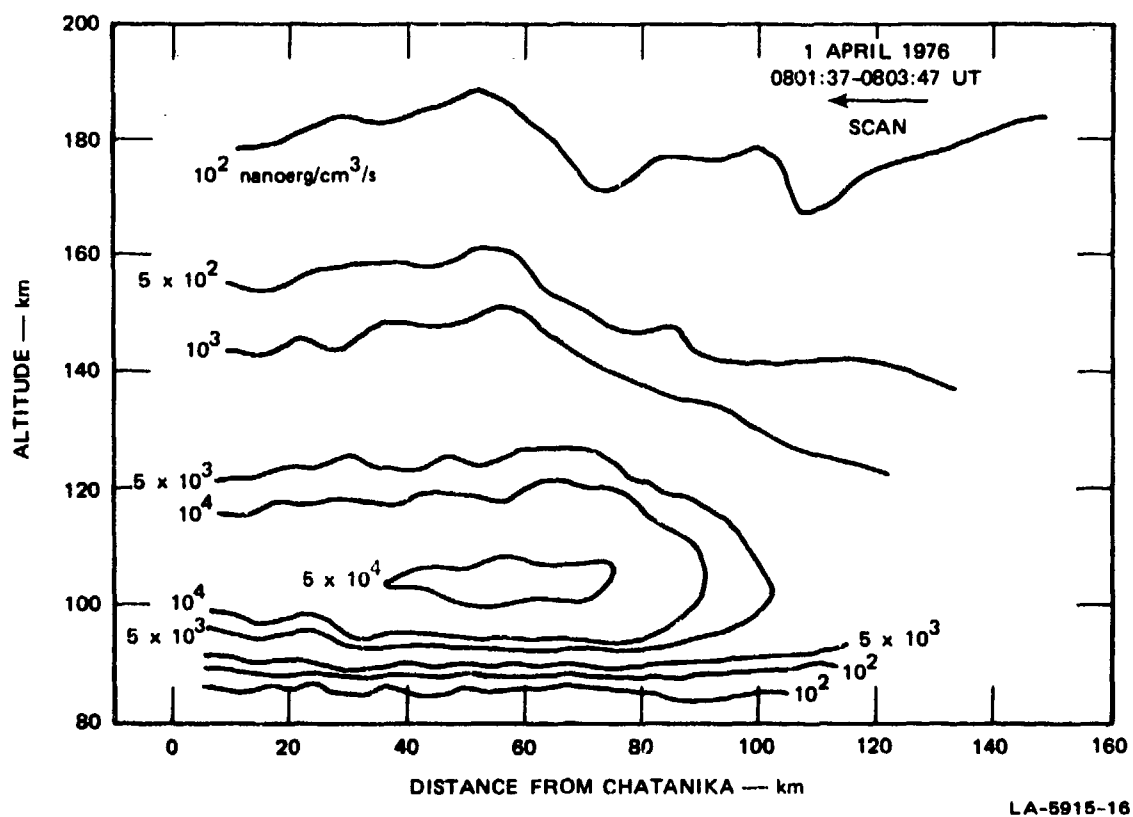


FIGURE 16 VOLUME ENERGY DEPOSITION RATE IN THE VICINITY OF THE HIRIS TRAJECTORY FOR THE PERIOD 0801:37 TO 0803:47 UT, 1 APRIL 1976

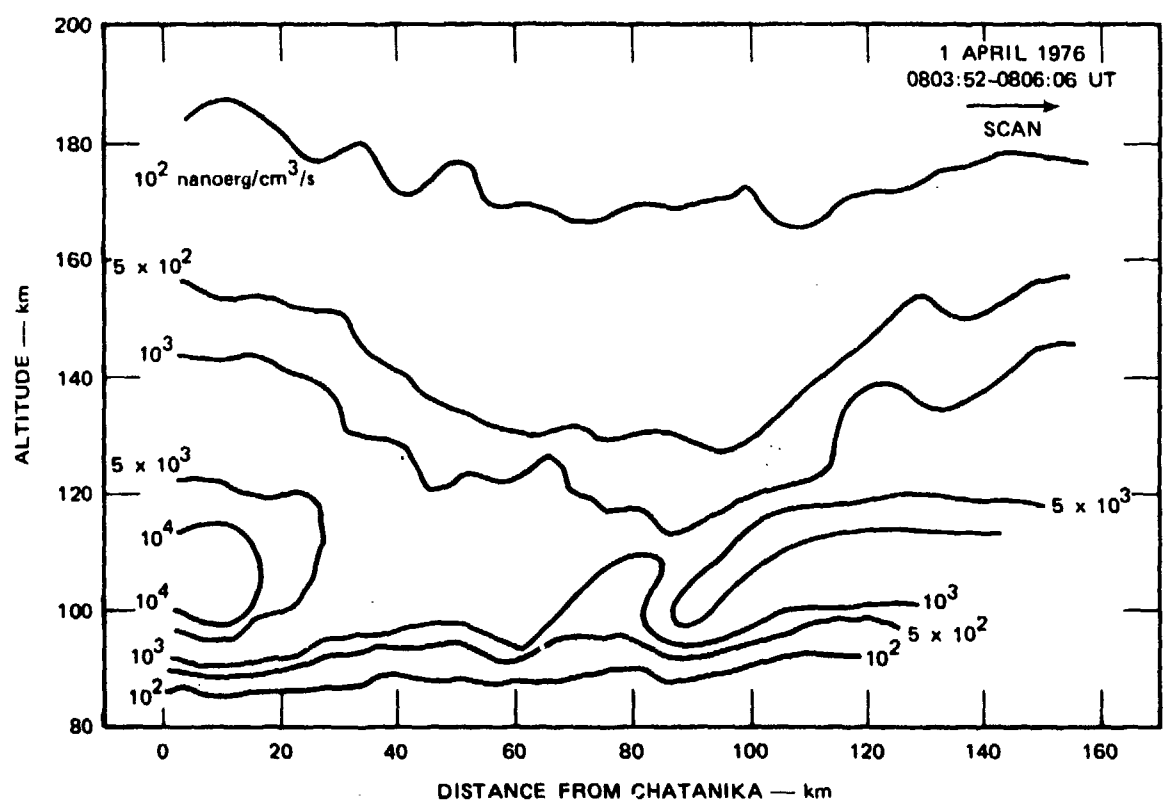


FIGURE 17 VOLUME ENERGY DEPOSITION RATE IN THE VICINITY OF THE HIRIS TRAJECTORY FOR THE PERIOD 0803:52 TO 0806:06 UT, 1 APRIL 1976

IV SUMMARY AND CONCLUSIONS

The HIRIS experiment took place on 1 April 1976, beginning at 0805:20 UT. The purpose of the experiment was to measure IR emissions in an aurorally disturbed ionosphere.

The Chatanika radar was operated in support of the rocket experiment from 0626 UT to 0821 UT. For a period of about 80 minutes prior to launch the radar was operated in a three-position mode and obtained prelaunch information on the transport quantities electric field, current density, and neutral wind. Just before launch the radar antenna was scanned twice in elevation to measure electron densities near the expected rocket trajectory. During the ionospheric traversal of the rocket, the radar was operated successively at two fixed positions providing near-intersection between the radar beam and the rocket trajectory.

Radar data acquired during the HIRIS experiment were later processed and are presented in this report. In general, the following results were obtained:

- Background electron densities in the vicinity of the rocket trajectory ranged between 3×10^4 and $3 \times 10^5/\text{cm}^3$. During the background measurement period (<0745 UT) the peak of the auroral-E layer appeared to be above the trajectory apogee, with electron densities at all altitudes fluctuating with time. Horizontal gradients in density were observed from about 0700 to 0730 UT and seemed consistent with a density enhancement moving geomagnetically west. During the elevation-scan measurements just prior to launch, the peak of the ionization layer varied from 100 to 120 km and ionization density continued to fluctuate with time.
- Vector quantities measured during the prelaunch background period were indicative of the active conditions present during the experiment. Conductivities, current densities, neutral winds, and electric fields all tended to be unipolar during the measurement period, but exhibited large and rapid fluctuations. Joule heating exhibited large peaks centered at about 0640 and 0730 UT.
- Electron densities along the rocket trajectory, as measured by the radar, were typically $\leq 2 \times 10^5/\text{cm}^3$. The rocket introduced some extraneous echoes into the radar data. These were easily recognized and interpreted properly.

- Energy spectra of precipitating electrons during the rocket flight had characteristic₂ energies of 1.5 to 3 keV and total energy fluxes of 6 to 10 ergs/cm²/s.

REFERENCES

1. M. J. Baron, "DNA Project 617 Radar: Auroral Ionospheric Measurements," Final Report, Contract DNA001-72-C-0076, SRI Project 1703, Stanford Research Institute, Menlo Park, California (January 1974).
2. M. J. Baron and N. Chang, "ICECAP 73A, Chatanika Radar Results," Technical Report 4, Contract DNA001-74-C-0167, SRI Project 3118, Stanford Research Institute, Menlo Park, California (September 1974).
3. A. Brekke, J. R. Doupnik, and P. M. Banks, "A Preliminary Study of the Neutral Wind in the Auroral E-Region," J. Geophys. Res., Vol. 78, pp. 8235-8250 (1973).
4. A. Brekke, J. R. Doupnik, and P. M. Banks, "Incoherent Scatter Measurements of E-Region Conductivities and Currents in the Auroral Zone," J. Geophys. Res., Vol. 79, p. 3773 (1974).
5. P. D. Perreault and M. J. Baron, "ICECAP '74--Chatanika Radar Results," Technical Report 6, Contract DNA001-74-C-0167, SRI Project 3118, Stanford Research Institute, Menlo Park, California (October 1975).
6. V. B. Wickwar, M. J. Baron, and R. D. Sears, "Auroral Energy Input from Energetic Electrons and Joule Heating at Chatanika," J. Geophys. Res., Vol. 80, No. 31, pp. 4364-4367 (1975).
7. P. D. Perreault, R. R. Vondrak, and T. M. Watt, "ICECAP '75--Chatanika Radar Results," Technical Report 7, Contract DNA001-74-C-0167, SRI Project 3118, Stanford Research Institute, Menlo Park, California (August 1976).
8. T. M. Watt, "Chatanika Radar Results During the EXCEDE Experiment," Technical Report 8, Contract DNA001-74-C-0167, SRI Project 3118, Stanford Research Institute, Menlo Park, California (September 1976).

DISTRIBUTION LIST

DEPARTMENT OF DEFENSE

Director
Defense Advanced Research Proj. Agency
ATTN: Nuclear Monitoring Research
ATTN: Strategic Tech. Office

Defense Documentation Center
Cameron Station
12 cy ATTN: TC

Director
Defense Intelligence Agency
ATTN: DI-7D
ATTN: DT-1, Current Intel. Group

Director
Defense Nuclear Agency
ATTN: STSI, Archives
3 cy ATTN: STTL, Tech. Library
ATTN: DDST
3 cy ATTN: RAAE

Dir. of Defense Research & Engineering
Department of Defense
ATTN: S&SS (OS)

Commander
Field Command
Defense Nuclear Agency
ATTN: FCPR

Director
Interservice Nuclear Weapons School
ATTN: Document Control

Chief
Livermore Division, Field Command, DNA
Lawrence Livermore Laboratory
ATTN: FCPRL

DEPARTMENT OF THE ARMY

Commander/Director
Atmospheric Sciences Laboratory
US Army Electronics Command
ATTN: DISEL-BL-SY-S, F. E. Niles

Director
BMD Advanced Tech. Center
Huntsville Office
ATTN: ATC-T, Melvin T. Capps
ATTN: ATC-O, W. Davies

Commander
Harry Diamond Laboratories
ATTN: DRXDO-NP, Francis N. Wimenitz
ATTN: DRXDO-TI, Mildred H. Weiner

Commander
US Army Foreign Science & Tech. Center
ATTN: P. A. Crowley
ATTN: R. Jones

Commander
US Army Nuclear Agency
ATTN: MONA-WE, J. Berberet

DEPARTMENT OF THE ARMY (Continued)

Chief
US Army Research Office
ATTN: CRDARD-P, Robert Mace

DEPARTMENT OF THE NAVY

Chief of Naval Research
Navy Department
ATTN: Code 461

Commander
Naval Ocean Systems Center
ATTN: Code 2200

Director
Naval Research Laboratory
3 cy ATTN: Code 7701, Jack D. Brown
ATTN: Code 7127, Charles Y. Johnson
ATTN: Code 2600, Tech. Lib.
ATTN: Code 7730, Edgar A. McClean
ATTN: Code 7750, Darrell F. Strobel
ATTN: Code 7750, Wahab Ali
ATTN: Code 7750, J. Davis
ATTN: Code 7750, Paul Julienne
ATTN: Code 7700, Timothy P. Coffey

Commander
Naval Surface Weapons Center
ATTN: Code WA501, Navy Nuc. Prgms. Off.

DEPARTMENT OF THE AIR FORCE

AF Geophysics Laboratory, AFSC
ATTN: OPI, R. Walker
ATTN: LKB, Kenneth S. W. Champion
ATTN: OPR, James C. Ulwick
ATTN: OPI, R. McClatchey
ATTN: LKD, Rocco S. Narcisi
ATTN: OP, John S. Garing
ATTN: OPI, E. Loewenstein
ATTN: SUOL, Research Lib.
ATTN: OPR, Alva T. Stair
ATTN: OPR, Harold Gardner
ATTN: OPR, Hervey P. Gauvin

AF Weapons Laboratory, AFSC
ATTN: DYC, Capt L. Wittwer
ATTN: SUL
ATTN: DYC, John M. Kamm
ATTN: DYM, Major T. Johnson

AFTAC
ATTN: TF/Maj Wiley
ATTN: TN

Commander
Foreign Technology Division, AFSC
ATTN: TDPSS, Kenneth N. Williams

Commander
Rome Air Development Center, AFSC
ATTN: EMTLD, Doc. Library

SAMSO/SZ
ATTN: SZJ, Major Lawrence Doan
ATTN: SZJ, Lt Col David Golob

ENERGY RESEARCH & DEVELOPMENT ADMINISTRATION

EG&G, Inc.
Los Alamos Division
ATTN: Document Control

Los Alamos Scientific Laboratory
ATTN: Doc. Con. for R. F. Taschek
ATTN: Doc. Con. for Eric Jones
ATTN: Doc. Con. for John S. Malik

Sandia Laboratories
ATTN: Doc. Con. for A. Dean Thornbrough,
Org. 1245
ATTN: Doc. Con. for 3141 Sandia Rpt. Coll.

DEPARTMENT OF DEFENSE CONTRACTORS

Aerospace Corporation
ATTN: Irving M. Garfunkel
ATTN: V. Josephson

AVCO-Everett Research Laboratory, Inc.
ATTN: C. W. Rosenberg, Jr.

The Boeing Company
ATTN: Glen Keister

Brown Engineering Company, Inc.
ATTN: N. Passino

University of Denver
Colorado Seminary
Denver Research Institute
ATTN: Sec. Officer for David Murcay
ATTN: Sec. Officer for Mr. Van Zyl

General Electric Company
Space Division
Valley Forge Space Center
ATTN: J. Burns
ATTN: M. Linevsky
ATTN: M. H. Bortner, Space Sci. Lab.

General Electric Company
TEMPO-Center for Advanced Studies
ATTN: Don Chandler
ATTN: L. Ewing
ATTN: DASIAC
ATTN: Tim Stephens

General Research Corporation
ATTN: John Ise, Jr.

Geophysical Institute
University of Alaska
ATTN: Technical Library
ATTN: Neal Brown
ATTN: T. N. Davis

HSS, Inc.
ATTN: Donald Hansen

Institute for Defense Analyses
ATTN: Ernest Bauer
ATTN: Hans Wolfhard

IRT Corporation
ATTN: E. DePlomp

DEPARTMENT OF DEFENSE CONTRACTORS (Continued)

Johns Hopkins University
Applied Physics Laboratory
ATTN: Document Librarian

Kaman Sciences Corporation
ATTN: R. J. Bittner
ATTN: P. Jesson

Lockheed Missiles and Space Company, Inc.
ATTN: Richard G. Johnson, Dept. 52-12
ATTN: Martin Walt, Dept. 52-10
ATTN: Robert H. Au
ATTN: John Kumer
ATTN: Robert D. Sears, Dept. 52-14

Mission Research Corporation
ATTN: F. Fajen
ATTN: Dave Sowle
ATTN: Conrad L. Longmire
ATTN: M. Scheibe
ATTN: D. Archer
ATTN: Ralph Kilt

Photometrics, Inc.
ATTN: Irving L. Kofsky

Physical Dynamics, Inc.
ATTN: A. Thompson

University of Pittsburgh of the Comwlt. Sys. of
Higher Education
Cathedral of Learning
ATTN: Frederick Kaufman
ATTN: Manfred A. Biondi
ATTN: Wade L. Fite

The Trustees of Princeton University
Forrestal Campus Library
ATTN: F. W. Perkins, Plasma Physics Lab.

R & D Associates
ATTN: Robert F. Lelevier
ATTN: Forrest Gilmore
ATTN: R. P. Turco
ATTN: H. A. Ory

The Rand Corporation
ATTN: James Oakley

Science Applications, Inc.
ATTN: Daniel A. Hamlin
ATTN: Robert W. Lowen
ATTN: Lewis M. Linson
ATTN: D. Sachs

Space Data Corporation
ATTN: Edward F. Allen

Stanford Research Institute
ATTN: Robert S. Leonard
ATTN: Ronald White
ATTN: Alan Burns
ATTN: Ray L. Leadebrand
ATTN: James R. Peterson
ATTN: J. G. Depp
ATTN: Walter G. Chestnut
ATTN: L. L. Cobb
ATTN: Felix T. Smith
ATTN: E. J. Fremouw
ATTN: Theodore M. Watt

DEPARTMENT OF DEFENSE CONTRACTORS (Continued)

TRW Systems Group

ATTN: R. K. Plebuch, RI-2078
ATTN: R. Watson, RI-1096
ATTN: J. F. Frlichtenicht, RI-1196

DEPARTMENT OF DEFENSE CONTRACTORS (Continued)

Visidyne, Inc.

ATTN: T. C. Degges
ATTN: Oscar Manley
ATTN: J. W. Carpenter
ATTN: Henry J. Smith